Azbel resonances

1991 J. Phys.: Condens. Matter 3 9055

(http://iopscience.iop.org/0953-8984/3/46/007)

J. Phys.: Condens. Matter 3 (1991) 9055–9065. Printed in the UK

Azbel resonances

Chaitali Basu†, Abhijit Mookerjee†, Asok K Sen‡ and Prabhat K Thakur‡

† S N Bose National Centre for Basic Sciences, DB 17, Sector I, Salt Lake City, Calcutta 700064, India

‡ Saha Institute for Nuclear Physics, AF, Sector I, Bidhannagar, Calcutta 700064, India

Received 23 April 1991

Abstract. Although almost all states are localized in random chains, specific transmitting states exist at random energies. We study the transmittance in the vicinity of these resonances. We also study the transmittances at these resonances and carry out a multifractal analysis on them. The transmittances at resonance seem to have characteristics of both extended and localized states.

1. Introduction

It has been known for some time that in tight-binding one-dimensional chains with short-ranged overlap integrals, the electronic spectrum is a dense point set, almost all of which supports exponentially localized states. The existence of a few transmitting states has also been known for some time. These are the so-called *stochastic resonances* or *Azbel resonances* (Azbel 1983a, b, 1984, Azbel and Rubinstein, 1983). Pendry (1987) examined the reasons for the existence of these resonant states. He speculated that these states could be necklace states, i.e. a linear combination of a number of localized states almost degenerate in energy, but whose centres of localization are at different parts of the chain. They have sufficient overlaps between themselves and together span the chain. Azbel and Soven (1983) had earlier estimated the width of these resonances and the way in which these scale with the sizes of the chains.

2. Formalism

Since the width of the Azbel resonances decreases with length as $\exp(-2L/\xi)$ where ξ is a measure of the localization length, the search for Azbel resonances begins with quite small chains. For small chains, states at several energies will show a large transmittance. Many of these are actually localized states whose localization lengths are larger than the chain length. As we increase the length of the chain, most of these states no longer show non-zero transmittance. However, even at quite large lengths, some transmitting states remain. These are the Azbel resonances. The neighbourhood of these energies are then searched for very large lengths carefully and at a very fine energy mesh to locate the position of the resonances.

0953-8984/91/469055 + 11 $03.50

In this work, for the small and moderately long chains we use the vector recursion technique of Godin and Haydock (1988) to examine the transmittances. For the very long chains, as the vector recursion technique is rather slow, we use the transfer matrix method to estimate the transmittances.

The basic model for our system is the so-called Anderson model with diagonal disorder:

$$H = \sum_n \varepsilon_n \Phi_n^\dagger \Phi_n + \sum_n (V_{n+1} \Phi_{n+1}^\dagger \Phi_n + V_n \Phi_n^\dagger \Phi_{n+1}). \tag{1}$$

For diagonal disorder, $\varepsilon_n = \delta(\xi_n - 0.5)$ and all the $V_n = 1$. The ξ_n-values are *independent* random variables uniformly distributed between 0 and 1. δ is a measure of the strength of the disorder in the system and the energy is scaled in units of V in this case.

We shall establish the existence of Azbel resonances in the Anderson model. We shall also carry out a multifractal analysis of the transmittances in order to attempt to differentiate between extended, localized and Azbel states.

The sample will be of length $2N$ and described by a Hamiltonian

$$H_{\text{sample}} = \sum_{n=1}^{2N} [\varepsilon_n \Phi_n^\dagger \Phi_n + V(\Phi_{n+1}^\dagger \Phi_n + \Phi_n^\dagger \Phi_{n-1})]. \tag{2a}$$

To the two ends of this chain at $n = 1$ and $n = 2N$ we attach elementary, perfectly conducting semi-infinite leads. The purpose of the leads is to bear the incoming, reflected and transmitted waves:

$$H_{\text{in}} = \sum_{n=-\infty}^{0} [\varepsilon' \Phi_n^\dagger \Phi_n + V'(\Phi_{n+1}^\dagger \Phi_n + \Phi_n^\dagger \Phi_{n+1})] \tag{2b}$$

$$H_{\text{out}} = \sum_{n=2N}^{\infty} [\varepsilon'' \Phi_n^\dagger \Phi_n + V''(\Phi_{n+1}^\dagger \Phi_n + \Phi_n^\dagger \Phi_{n+1})]. \tag{2c}$$

For simplicity we take $\varepsilon' = \varepsilon'' = \varepsilon$ and $V' = V'' = 1$. The solutions of the Schrödinger equation in the two leads are known. These are travelling Bloch waves of the form

$$\Psi_{\text{leads}} = \sum_n \psi_n \Phi_n^\dagger \tag{3}$$

with $\psi_n = A \exp(\pm in\theta)$.

As the wave travels through the lead, its phase θ changes from one site to the next. In the elementary, perfectly conducting leads this change is determinate: $\cos\theta = E/2V$ where E is the energy of the incoming wave.

In the vector recursion technique (Godin and Haydock 1988) we change to a new *vector basis* with annihilation operators

$$\Phi_n = \begin{pmatrix} \varphi_n \\ \\ \varphi_{2N+1-n} \end{pmatrix}.$$

We choose the basis such that the sample Hamiltonian is block tridiagonal. Details of the numerical procedure has been described in recent work (Basu *et al* 1991):

$$B_{n+1}^\dagger \Phi_{n+1} = \Phi_n(EI - A_n) - \Phi_{n-1} B_n. \tag{4}$$

The Schrödinger equation satisfies an equation identical with (4) with the wavefunction vector amplitudes

$$\Psi_n = \begin{pmatrix} \psi_n \\ \psi_{2N+n-1} \end{pmatrix}.$$

We have to supply the boundary conditions at the joints. An incoming wave $\Sigma_n \exp(in\theta)\ \varphi_n^\dagger$ travels to the right along the incoming lead. As it reaches the sample, it is scattered. A *reflected* wave $\Sigma_n r(E) \exp(-in\theta)\ \varphi_n^\dagger$ travels back along the same lead, while a *transmitted* wave $\Sigma_n t(E) \exp(in\theta)\ \varphi_n^\dagger$ travels in the other lead. $r(E)$ and $t(E)$ are the reflection and transmission coefficients. The boundary conditions at the lead joints are given by

$$\Psi_0 = \begin{pmatrix} 1 + r(E) \\ t(E) \end{pmatrix}$$

and

$$\Psi_1 = \begin{pmatrix} \exp(i\theta) + r(E) \exp(-i\theta) \\ t(E) \exp(-i\theta) \end{pmatrix}.$$

Since the length of the scattering part is finite, we have another boundary condition. The *vector chain* terminates after N steps, so that $\gamma_{N+1} = 0$. From the boundary conditions we immediately obtain an expression for the scattering **S**-matrix:

$$\mathbf{S}_N = \begin{pmatrix} rt \\ t'r' \end{pmatrix} = -[X_{N+1} + Y_{N+1} \exp(-i\theta)]^{-1}(X_{N+1} + Y_{N+1} \exp(i\theta)).$$

The *transmittivity* $T(E)$ is $|t(E)|^2$ and the *reflectivity* $R(E)$ is $|r(E)|^2$.

In the calculation of the reflection and transmission coefficients, $r(E)$ and $t(E)$ respectively, we first fix the energy E and then use the boundary conditions (9) and (11) to obtain two equations in these variables. Conversely, if we wish to locate the Azbel resonances at which $T(E)$ is almost 1 and $R(E)$ is almost 0, we substitute these in (9) and use the boundary condition (11) as an equation in E. The solutions of this, if they lie within the band, are the Azbel resonant energies. For a fixed size $2N$ of the sample, we can always numerically show the existence of the Azbel resonances. It may be noted that this is not a proof of the existence of such resonances at infinite sizes.

It may be mentioned that for large system sizes (greater than 10^3) we have used a recursion technique with single-site transfer matrices (see, e.g., Liu and Chao 1986) as opposed to the vector recursion technique referred to above. This method has the advantage of being exponentially faster when one keeps on adding length elements at the end of the original chain but has the disadvantage of being limited to one dimension only.

The transmitted wave is $\Psi_N(E) = t_N \Psi_0(E)$, so that $t_N(E)$ carries the information about the relative amplitude and phase of the transmitted wave for a sample of size N. The set $\{T_N(E) = |t_N(E)|^2\}$ then represents a set of measurements on a collection of chains of varying sizes $\{n\}$. The chain of size $n + 1$ is identical with the chain of size n up to the nth element. Note that this set is different in essence from the wavefunction amplitudes at different sites of a single isolated chain. For the multifractal analysis we shall use this set of transmittances properly normalized. Again, this analysis is different in essence from the multifractal analysis of wavefunction amplitudes for isolated chains.

The Qth moment of this distribution for any real value of Q is

$$Z(Q) = \sum_{n=1}^{2N} P_n^Q \tag{5}$$

where $P_n = T_n(E)/T$ and $T = \Sigma_n T_n(E)$. This Qth moment is also called the partition function of the distribution (Halsey *et al* 1986).

The indices $\tau(Q)$, α and $f(\alpha)$ are defined by the asymptotic behaviours

$$Z(Q) \sim N^{-\tau(Q)} \qquad P_N \sim N^{-\alpha}$$

and the fraction of atoms having exponents between α and $\alpha + d\alpha$ is $N^{f(\alpha)}$.

The three exponents $\tau(Q)$, α and $f(\alpha)$ are related to each other by

$$\begin{aligned}\tau(Q) &= \alpha Q - f(\alpha) \\ &= (Q-1)D_Q.\end{aligned} \tag{6}$$

D_Q is referred to as the generalized (Rényi) dimension of index Q. As can be easily seen from (6), $\alpha = d\tau/dQ$. The curvature of the $f(\alpha)$ curve is

$$C = \left(\frac{d^2 f}{d\alpha^2}\right)_{\alpha=\alpha_0} = \frac{\frac{1}{2}}{(d\tau/dQ^2)_{Q=0}}.$$

Non-divergence of the curvature is a signature of genuine multifractality.

For numerical facility, α and $f(\alpha)$ can also be computed directly, avoiding numerical differentiation (Chhabra and Jensen 1989):

$$\alpha = -Z'(Q)/[Z(Q)\ln(2N)] \qquad f(\alpha) = [1/\ln(2N)]\{\ln[Z(Q)] - QZ'(Q)/Z(Q)\}$$

and the expression for C (Godrèche and Luck 1990) is

$$1/C = [1/\ln(2N)][Z'(0)^2/Z(0)^2 - Z''(0)/Z(0)]. \tag{7}$$

3. Results and discussion

We have studied transmittance versus the energy E of the incoming electron numerically to obtain the resonant states. The width of the resonance peaks becomes narrower as the sample length is increased. Figure 1 shows the position of the Azbel resonance for an Anderson model with purely diagonal disorder. The resonance peak becomes sharper as the length is increased from 30 000 (in figure 1(a)) to 40 000 (in figure 1(b)). The states over a very narrow energy region are transmitting while all the rest are localized. As seen in these figures, the resonant state persists with increasing length but the energy at which resonance occurs tends to shift. For the length 30 000 the resonance is at $E = -0.3344$ while for the length 40 000 it occurs at $E = -0.3385$.

Figure 2 shows the transmittance plot for Azbel resonant states. In both the length scales, the transmittance remains finite in most parts of the sample size. The sample is connected to perfectly conducting leads on both sides. So the transmittance at the incoming end is always equal to 1. Figure 2(a) shows the transmittance at an Azbel resonance in a sample of length 30 000, while figure 2(b) shows the transmittance at the shifted Azbel resonance in a sample of length 40 000. Figure 2(c) shows the same for a localized state in a sample of length 100 000. Here the incoming lead has a transmittance equal to 1 and this falls off exponentially as the wave travels through the sample. The

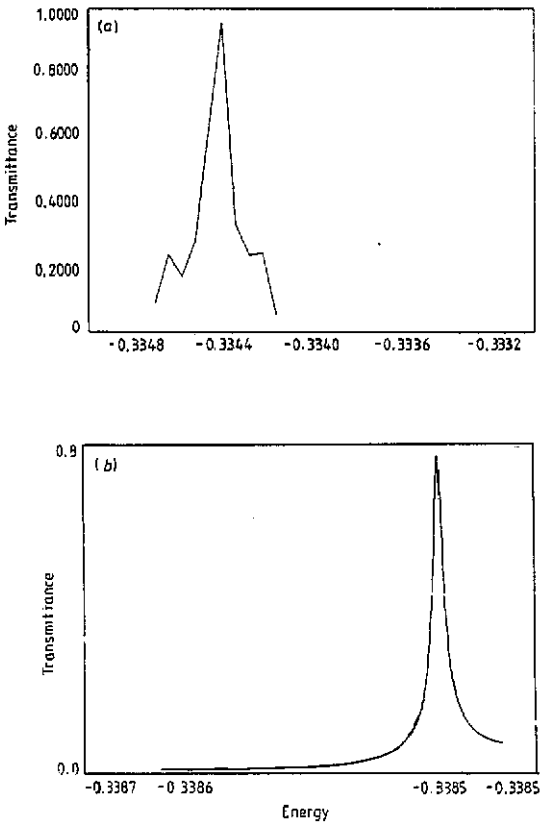

Figure 1. Transmittance versus energy (a) for a chain of size 30 000 and (b) for a chain of size 40 000.

wave is localized within a small length region from the incoming sides. In contrast with figures 2(a) and 2(b) except for a small mesoscopic regime the transmittance rapidly goes to zero.

The transmittances in these disordered samples show very large fluctuations from size to size and are highly fragmented. One of the powerful methods of analysing such fragmented objects is through the multifractal analysis described earlier in section 2 (Halsey *et al* 1986).

Figure 3 shows a plot of $\tau(Q)$ versus Q for all three types of state: extended, localized and Azbel. For the extended state, the graph is a straight line with an almost constant slope denoted by the broken line here. For a localized state, the graph consists of two separate straight lines of different slopes for positive and negative values of Q, continuous at $Q = 0$. This is shown by the chain curve. For the Azbel state, the graph is a straight line with a constant slope. Its slope is different from the extended case. It is denoted by the full curve in the figure. For extended states, $P_n \sim 1/N$, so that $Z(Q) \sim N^{1-Q}$. This leads to $\tau(Q) = Q - 1$, which is a straight line with unit slope. For localized states, P_n is significantly non-zero only in an interval of size L. For positive and increasing Q the size of the interval over which P_n^Q is significantly non-zero $(L(Q))$ decreases as Q increases. $Z(Q) \sim L^{1-Q}$. $\tau(Q) \sim (1 - Q)\{\ln[L(Q)]/\ln N\}$. The slope of this curve decreases from unity with increasing positive Q-value. For negative and large

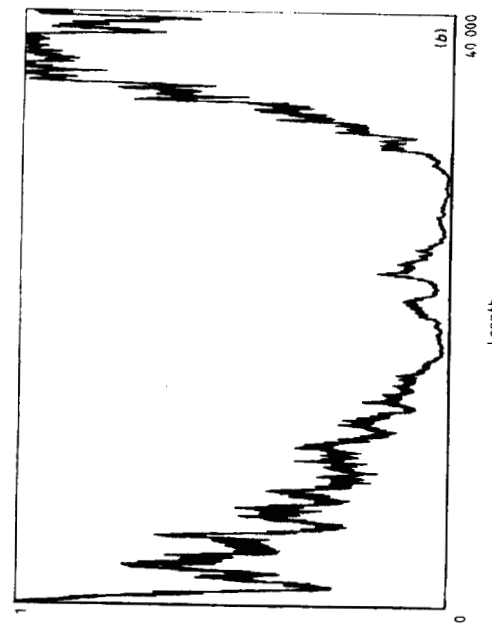

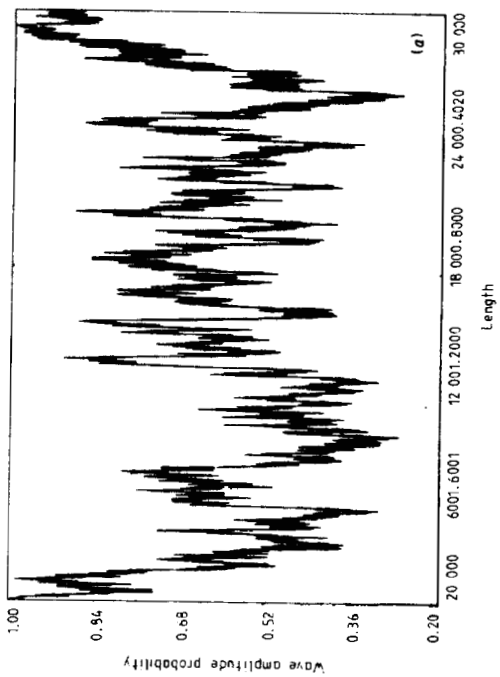

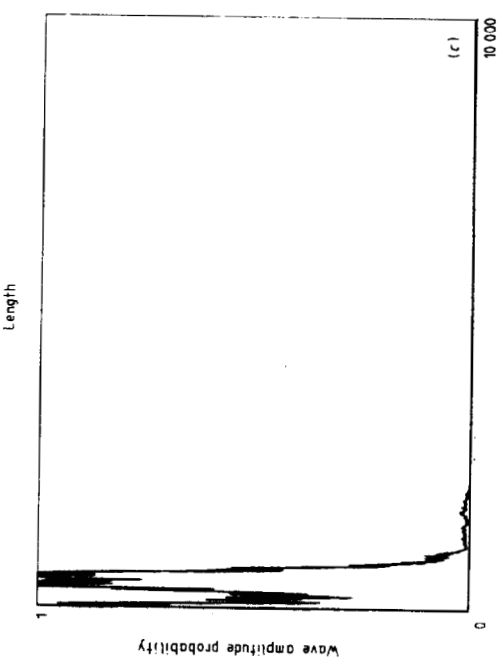

Figure 2. Transmittance plotted against chain length (*a*) for an Azbel resonant energy in a chain of length 30 000, (*b*) for the shifted Azbel resonant energy in a chain of size 40 000 and (*c*) for a localized state in a chain of length 100 000.

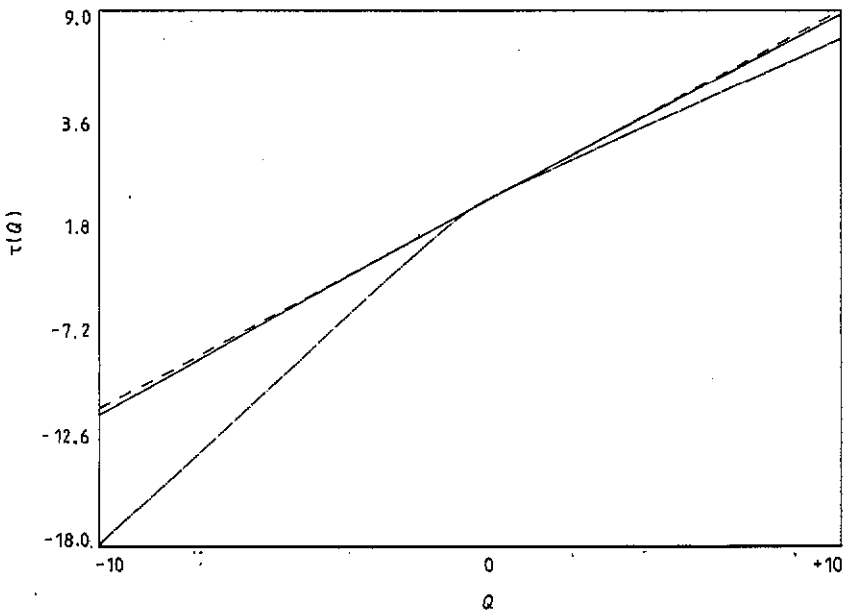

Figure 3. The scaling index $\tau(Q)$ versus Q for extended localized and Azbel states.

$Q = -Q'$, $P_n^Q = P_n^{-Q'}$ is now large over that interval over which P_n is almost zero. If we estimate P_n in the intervals of width ε, then $Z(Q) \sim N'(\varepsilon)^{-Q'} \sim N^{-\tau}$:

$$\tau(Q') = Q'[(\ln \varepsilon)/(\ln N)] - (\ln N')/(\ln N)$$

where $N' = N - L(Q)$. This is large and negative as ε is small. These characteristics are clear in figure 3. Particularly in this respect the Azbel states resemble extended states. We expect this, as the nature of the localized states, i.e. non-zero in a small interval, which is reflected in the $\tau(Q)$ versus Q graphs is not shared by the Azbel states. However, the slope for the Azbel state curve is not unity, since the states do not possess translational symmetry and $P_i \neq (1/N)$.

Figure 4 shows $f(\alpha)$ versus α curves for extended, localized and Azbel states at different sample lengths. Since numerical work is always carried out on finite samples, the study of the asymptotic behaviour of the α versus $f(\alpha)$ curves as the size increases is very important.

Figure 4(a) shows the graph for an extended state. The state is for $\delta = 0.01$ and $E = 0$. For one dimension no true extended states exist for $\delta > 0$ but, for this weak disorder and energy, the state has a localization length much greater than 30 000, the maximum size taken, and for these lengths conveniently mimics extended states. For almost all values of Q, $f(\alpha) \sim 1$ and $\alpha \sim 1$. The interesting point here is the behaviour of the graphs as we increase the length of the sample. For a sample of length 10 000 the $f(\alpha)$ versus α curve is the outermost full curve. The curve converges inwards as the length of the sample increases to 20 000 and 30 000 respectively. For larger lengths the curve will converge to the point (1, 1).

Figure 4(b) shows the graph for a localized state. Here the curves move outwards as we increase the length scale. The interesting point to observe is that the densities of points near $\alpha_{\min}$ and $\alpha_{\max}$ are very high whereas the intermediate region is sparsely

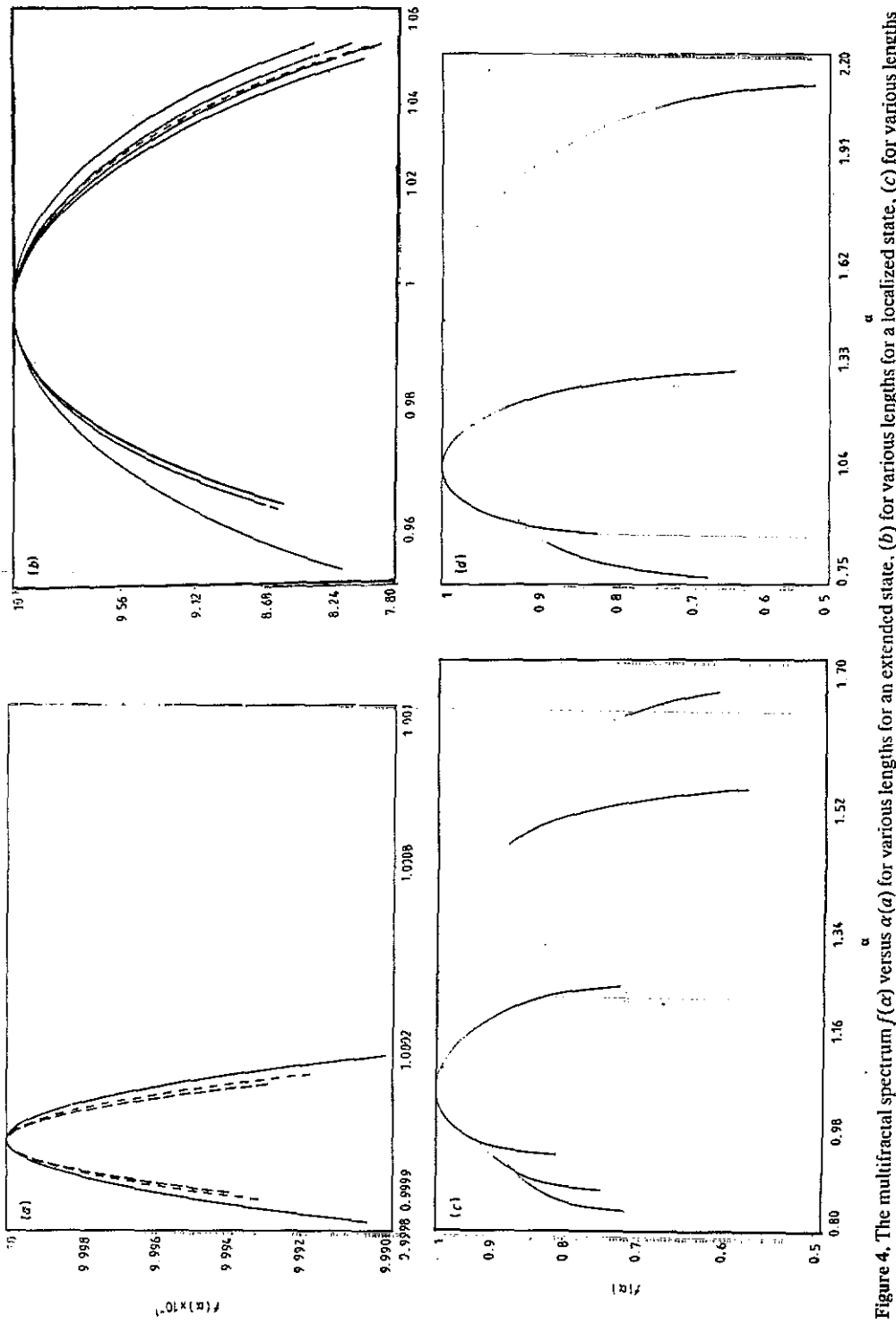

Figure 4. The multifractal spectrum $f(\alpha)$ versus $\alpha(a)$ for various lengths for an extended state, (*b*) for various lengths for a localized state, (*c*) for various lengths for an Azbel state and (*d*) for a localized state and an Azbel state.

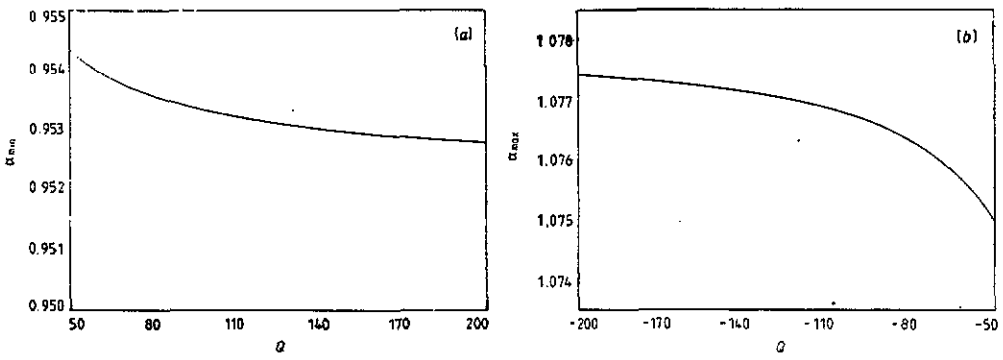

Figure 5. (*a*) α_{min} versus Q; (*b*) α_{max} versus Q.

populated. This indicates clearly the fact that, for exponential localization, α_{min}'s becoming smaller and smaller corresponds to a large probability (which should ideally be about unity) for getting the electron within the localization length. α_{max} becomes larger and larger, implying that probability decays exponentially for lengths larger than the localization length. The asymptotic convergence is at the point (0, 0) and (∞, 1).

Figure 4(*c*) shows the graph for an Azbel state. Here the graphs are spread out, with a significant $\alpha_{max} - \alpha_{min}$ compared with the extended state although the peak still occurs at ($\geqslant$1, 1). The behaviour of the graph with increasing lengths is, however, significantly different from the extended or localized case. Here α_{max} and α_{min} oscillate about some mean position. The graph narrows significantly as the length is increased from 5000 to 10 000. However, after that the increase in length scale results in a close overlap on the α_{min} side but a small oscillation on the α_{max} side. As seen with increasing N the Azbel state shows finite (α_{min}, α_{max}). Unlike the extended state, $\alpha_{min} \neq \alpha_{max}$ and, unlike localized states, α_{max} is finite. The true multifractal nature of the Azbel states resemble more closely the critical states in incommensurate systems.

Figure 4(*d*) compares the α versus $f(\alpha)$ curves of a localized state and an Azbel state. As seen, the density of points in the curve for the Azbel state is uniform whereas for the localized state the points are concentrated at the two ends.

Figure 5 shows the behaviour of α_{min} and α_{max} for an Azbel resonant state with increasing Q. Q is varied from 50 to 200 in figure 5(*a*). α_{min} decreases in the beginning but approaches a constant value for $Q \geqslant 110$. Figure 5(*b*) shows the Q variation from -50 to -200 to estimate α_{max}. As expected, α_{max} increases with increase in negative Q-value and reaches a fixed value from about $Q = -120$.

Figure 6 shows the behaviour of $f(\alpha_{min})$ and $f(\alpha_{max})$ with increasing Q for Azbel resonant state. Figure 6(*a*) shows the Q variation from 50 to 200 to find $f(\alpha_{min})$. Figure 6(*b*) shows the Q variation from -50 to -200 to find $f(\alpha_{max})$. f decreases for both large positive and large negative values of Q. $f(\alpha_{max})$ decreases more sharply than $f(\alpha_{min})$, going towards zero for large negative Q-values. However, any further increase in Q-value causes numerical instability and, to overcome this, quadruple precision (not available to us) has to be used.

Figure 7 shows the curvature for the multifractal analysis of the transmittances at Azbel resonance. Figure 7(*a*) gives the curvature C versus $2N$, the sample size. Figure 7(*b*) gives the curvature C versus $1/2N$ (Godrèche and Luck 1990). As seen from the

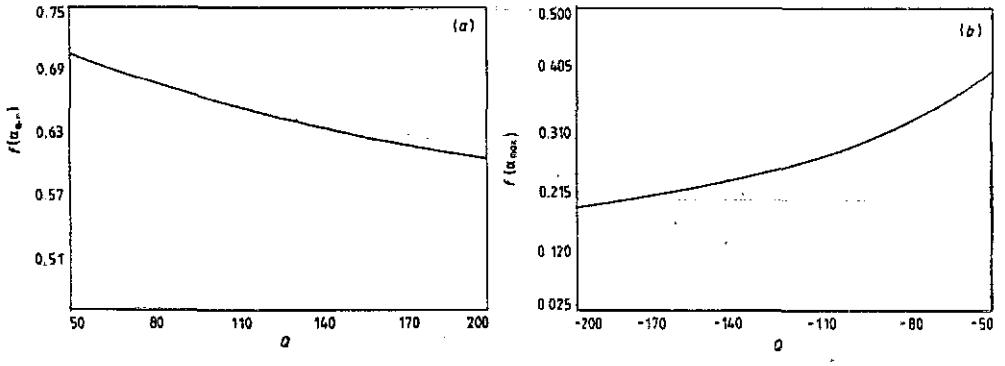

Figure 6. (*a*) $f(\alpha_{min})$ versus Q; (*b*) $f(\alpha_{max})$ versus Q.

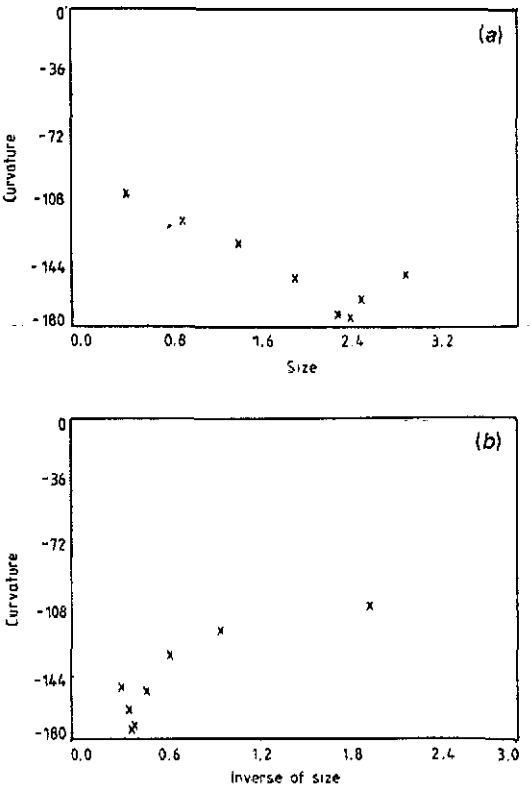

Figure 7. The curvature C versus (*a*) the chain size and (*b*) the inverse of the chain size.

curves, they are not divergent, indicating that the transmittances at Azbel resonance is truly multifractal in nature.

The important parameters noted for the Azbel resonance are the following.

(i) At $Q = 0$, $\alpha = \alpha_0$ corresponding to the top of the $f(\alpha)$ curve. This α_0 is the strength of a generic singularity. Here $f = 1$ but $\alpha_0 = 1.003\,27$ for a sample length of

30 000 and $\alpha_0 = 1.045\,92$ for a sample length of 40 000. As $\alpha_0 > 1$, the set of transmittances is genuinely multifractal (Godrèche and Luck 1990).

(ii) α_{min} and α_{max} converge to constant values for large Q-values as already discussed. $\alpha_{min} = 0.9530$ and $\alpha_{max} = 1.0774$.

(iii) At $Q = 1$, $\alpha = \alpha_1 = f(\alpha_1) = D_1$. This is called the dimension of the measure. Here $D_1 = 0.9968$ for $2N = 30\,000$ and $D_1 = 0.9653$ for $2N = 40\,000$.

In conclusion, Azbel resonant states exist for almost all configurations. The wavefunctions at these resonances are transmitting. The set of normalized transmittances at different sample sizes are multifractal in nature and resemble neither truly extended nor truly localized states. The wavefunction amplitudes show clumped behaviour. We propose to extend the multifractal analysis to the two-point correlation functions (Chhabra and Jensen 1990) to study this characteristic. This will be reported in a subsequent communication.

Acknowledgments

AM would like to record work done under project SP/S2/M-56/89 of the Department of Science and Technology, India. He would like especially to thank Dr G Ananthakrishna (IGCAR, Kalapakkam, India) for several important discussions. CB thanks CSIR for financial assistance during the period of work. PKT thanks Dr C K Majumdar for the computer facility received at the S N Bose National Centre For Basic Sciences.

References

Azbel M Ya 1983a *Phys. Rev.* B **27** 3852
—— 1983b *Phys. Rev.* B **28** 4106
—— 1983c *Solid State Commun.* **45** 527
—— 1984 *Phil. Mag.* B **50** 229
Azbel M Ya and Rubinstein M 1983 *Phys. Rev.* B **51** 836
Azbel M Ya and Soven P 1983 *Phys. Rev.* B **49** 831
Basu C, Mookerjee A, Sen A K and Thakur P K 1991 *J. Phys.: Condens. Matter* **3** 6041
Blumenfeld R and Aharony A 1989 *Phys. Rev. Lett.* **62** 2977
Chhabra A and Jensen V R 1989 *Phys. Rev. Lett.* **62** 1327
Godin T J and Haydock R 1988 *Phys. Rev.* B **41** 5237
Godrèche C and Luck J M 1990 *J. Phys. A: Math. Gen.* **23** 3769
Gupte N and Amritkar R E 1989 *Phys. Rev.* A **39** 5466
Halsey T C, Jensen M H, Kadanoff L P, Procaccia I and Shraiman B I 1986 *Phys. Rev.* A **33** 1141
Johansson M and Riklund R 1990 *Phys. Rev.* B **42** 8244
Liu Y and Chao K A 1986 *Phys. Rev.* B **34** 5247
Pendry J 1987 *J. Phys. C: Solid State Phys.* **20** 733